2024 Tenth Indian Control Conference (ICC)
9 - 11 December, 2024
IISER Bhopal, India

Temperature Control of a PEMFC by using Barrier Function Based Super-Twisting Sliding Mode Control

Tushar Meshram [1] and Jay Prakash Singh [2]

Abstract— **Hydrogen as a clean and sustainable energy carrier holds immense promise for addressing contemporary energy challenges. Proton Exchange Membrane Fuel Cells (PEMFC) represents a pivotal technology in the production of hydrogen through electrolysis of water. In this study, we explore the efficacy of two distinct control strategies-PI and Barrier function based super twisting Sliding Mode Control (BF-STSMC) in regulating the temperature of a PEMFC system. The control input which modulates the coolant flow rate is examined in response to variations in the current passing through the stack. Simulation results reveal significant insights into the performance of the mentioned control strategies. BF-STSMC approach demonstrates a shorter settling time and mitigates chattering highlighting its potential for efficient temperature regulation in PEMFC systems. The findings presented in this paper contribute to advancing our understanding of temperature control strategies in PEMFC systems and offer valuable insights for optimizing hydrogen production processes.**

I. INTRODUCTION

In the field of energy conversion and storage, PEMFC stand out as a promising technology [2] for clean hydrogen production. With the increasing demand for renewable energy sources and the imperative to reduce greenhouse gas emissions, PEMFC have attracted considerable interest due to their potential for efficient and environmentally friendly hydrogen generation. However, to fully exploit their capabilities, precise control of various operational parameters particularly temperature is needed.

Temperature regulation plays a pivotal role in the performance and longevity of a PEMFCs. The optimal operating temperature ensures enhanced efficiency [3], [4], electrolyte conductivity, and electrode kinetics, thereby maximizing the conversion efficiency of electrical energy into hydrogen. Moreover, maintaining a stable temperature mitigates the risk of thermal degradation and prolongs the lifespan of the cell components [5]. Traditionally, temperature control in a PEMFC has been achieved through conventional proportional-integral-derivative (PID) control methods [6]. While effective to some extent, these methods often face challenges in coping with nonlinear dynamics, uncertainties, and disturbances inherent in a PEMFC systems. As a result, there is a growing interest in exploring advanced control techniques to address these shortcomings and enhance the overall performance of a PEMFC systems.

Table 1. Different control techniques to control temperature of a PEMFC.

References	Control techniques used to control the temperature of a PEMFC
[7]	Higher order SMC
[8]	Sparrow search algorithm
[9]	MPC method
[10]	PI
[11]	Fuzzy
[12]	Predictive control
[13], [14]	Neural network
[15]	Disturbance deep reinforcement
[16]	Data driven method
This work	Barrier function-based ST-SMC

Table 1 show the previous work done on different control techniques for controlling the operating temperature of PEMFC. One such advanced control methodology that has shown promise in addressing the complexities of a PEMFC temperature control is BF-STSMC. BF-STSMC is a robust control technique known for its ability to handle system uncertainties and disturbances through the creation of a sliding surface, upon which the system dynamics are constrained. By continuously driving the system states towards this sliding surface, SMC ensures robust stability and performance even in the presence of external perturbations.

This research paper aims to investigate the application of BF-STSMC for temperature regulation in a PEMFC. Through theoretical analysis and simulation studies, the effectiveness of BF-STSMC in achieving precise and robust temperature control will be evaluated. Furthermore, the paper will explore the potential benefits of integrating SMC into PEMFC systems, including improved efficiency, enhanced durability, and greater reliability.

T. M. Meshram is with the Visvesvaraya National Institute of Technology, Nagpur, India (e-mail: tshrmshrm@gmail.com).

J. P. Singh, is with Visvesvaraya National Institute of Technology, Nagpur, India, 440010 (e-mail: jpsinghvnit@gmail.com).

II. MATHEMATICAL MODELLING OF A PEMFC

PEMFC operates on the principle of electrolysis, where an electric current is used to split water into hydrogen and oxygen [17]. In a PEMFC, a solid polymer electrolyte membrane facilitates the ion exchange process. When an electric current is applied, water molecules are dissociated at the membrane, with hydrogen ions (protons) migrating through the membrane to form hydrogen gas at the cathode, while oxygen is evolved at the anode. This technology, relying on the proton-conducting membrane, allows for a more efficient and compact electrolysis process, making PEMFCs a promising choice for hydrogen production in various applications. Figure 1 shows the electrolytic reaction diagram in PEMFC.

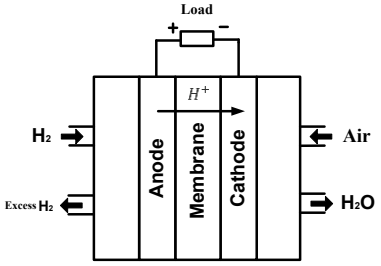


Figure 1: PEMFC electrolytic reaction diagram.

The template is used to format your paper and style the text. All margins, column widths, line spaces, and text fonts are prescribed; please do not alter them. You may note peculiarities. For example, the head margin in this template measures proportionately more than is customary. This measurement and others are deliberate, using specifications that anticipate your paper as one part of the entire proceedings, and not as an independent document. Please do not revise any of the current designations.

A. Voltage Modelling

The voltage of the cell (V_{cell}) in a Proton Exchange Membrane Fuel Cell (PEMFC) is determined by several factors including activation losses (V_{act}), ohmic losses (V_{ohm}), concentration losses (V_{con}), and the open-circuit voltage (E_n) [17].

N number of cells connected in series to form a stack, its equation is given by:

$\mathrm{V_{st}} = NV_{cell}$

The voltage equation is expressed as:

$$V_{cell} = E_n - V_{\text{act}} - V_{\text{ohm}} \quad (1)$$

The open-circuit voltage (E_n) [17] is the voltage of the cell when no current is flowing. It is dependent on temperature ($\mathrm{T_{st}}$), stack pressure (P), and the partial pressures of hydrogen ($\mathrm{P_{H_2}}$) and oxygen ($\mathrm{P_{O_2}}$).

$$E_n = 1.229 - (8.5 \times 10^{-4})(T_{\text{st}} - 298.15) + 4.308 \times 10^{-5}\mathrm{T_{st}} \times \left[\ln\left(\frac{\mathrm{P_{H_2}}}{\mathrm{P}}\right) + \frac{1}{2}\ln\left(\frac{\mathrm{P_{O_2}}}{\mathrm{P}}\right)\right] \quad (2)$$

Activation voltage loss (V_{act}) [17] accounts for the kinetic barriers associated with the electrochemical reactions. This component is calculated separately using a specified method.

$$\mathrm{V_{act}} = \xi_1 + \xi_2\mathrm{T_{st}} + \xi_3\mathrm{T_{st}}\ln(\mathrm{C_{O_2}}) + \xi_4\mathrm{T_{st}}\ln(\mathrm{I_{st}}) \quad (3)$$

Ohmic voltage loss (V_{ohm}) is due to the electrical resistance within the cell, including that of the electrolyte, membrane, and electrodes [17].

$$V_{\text{ohm}} = I_{\text{st}}\, R_{\text{int}} \quad (4)$$

where $R_{\text{int}} = \frac{r_M t_M}{A_{\text{active}}}$, and

$$r_M = \frac{181.6\left[1+0.03\left(\frac{I_{\text{st}}}{A_{\text{active}}}\right)+0.062\left(\frac{T_{\text{st}}}{303}\right)^2\left(\frac{I_{\text{st}}}{A}\right)^{2.5}\right]}{\left[\lambda-0.634-3\left(\frac{I_{\text{st}}}{A_{\text{active}}}\right)\right]\exp\left[4.18\left(\frac{T_{\text{st}}-303}{T_{\text{st}}}\right)\right]} \quad (5)$$

The ohmic voltage loss (V_{ohm}) in the voltage equation for a PEMFC is determined by several factors. Among these, r_M represents specific resistivity of the membrane experienced by protons, t_M signifies the thickness of the membrane, A_{active} denotes the active area of the cell, and λ represents the membrane water content. Fig. 2 represents equivalent circuit of a PEMFC cell from which can be represented in equation as;

$$\frac{dV_{act}}{dt} = \frac{i}{C_{dl}} - \frac{V_{act}}{R_{act}C_{dl}} \quad (6)$$

where C_{dl} is a double layer capacitance of one cell (F), R_{act} is a activation resistance and i is a cell current which is equal to stack current (I_{st}).

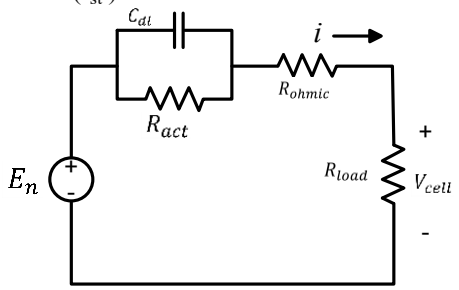


Figure 2: Equivalent circuit of a PEMFC cell.

B. Temperature Modelling

The stack's dynamic thermal model is established based on the law of energy conservation. This model considers various energy components involved in the system, including the total power ($\dot{\mathrm{Q}}_{\mathrm{tot}}$) generated by electrochemical reactions, the electric power ($\mathrm{P_{st}}$) consumed by the load, the thermal power extracted by the coolant ($\dot{\mathrm{Q}}_{\mathrm{cl}}$), and the thermal power losses by radiator ($\dot{\mathrm{Q}}_{\mathrm{loss}}$) [17]. The thermal model equation is expressed as:

$$m_{\mathrm{st}} C_{\mathrm{st}} \frac{dT_{\mathrm{st}}}{dt} = \dot{\mathrm{Q}}_{\mathrm{tot}} - \mathrm{P}_{\mathrm{st}} - \dot{\mathrm{Q}}_{\mathrm{cl}} - \dot{\mathrm{Q}}_{\mathrm{loss}} + d(t) \quad (7)$$

where, m_{st} is the mass of the stack, C_{st} is the specific heat capacity of the stack, $\frac{dT_{\mathrm{st}}}{dt}$ is the rate of change of temperature of the stack, $\dot{\mathrm{Q}}_{\mathrm{tot}}$ is the total power generated by electrochemical reactions, P_{st} is the electric power consumed by the load, $\dot{\mathrm{Q}}_{\mathrm{cl}}$ is the thermal power extracted by the coolant, $\dot{\mathrm{Q}}_{\mathrm{amb}}$ is the thermal power losses by radiator and $d(t) = \sin(2t) + \cos(2t)$ denotes any disturbances experience by the system.

The electrochemical reactions ($\dot{\mathrm{Q}}_{\mathrm{tot}}$) generated power is calculated as a function of the cell number (N), stack current (I_{st}), and total enthalpy change ($\Delta\mathrm{H}$) provided by the reaction gas:

$$\dot{\mathrm{Q}}_{\mathrm{tot}} = \frac{N I_{\mathrm{st}}}{2\mathrm{F}} \Delta\mathrm{H} \quad (8)$$

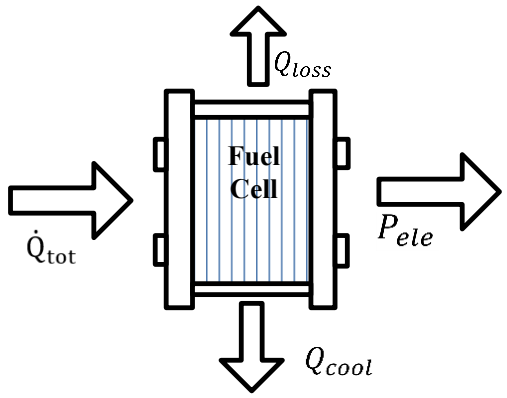


Figure 3: Energy balance model of a PEMFC.

The output power consumed by the load (P_{st}) is the product of the stack voltage (V_{st}) and stack current (I_{st}).

$$\mathrm{P}_{\mathrm{st}} = \mathrm{V}_{\mathrm{st}} \mathrm{I}_{\mathrm{st}} \quad (9)$$

The thermal power extracted by the cooling water ($\dot{\mathrm{Q}}_{\mathrm{cl}}$) is directly in reaction with flow rate of coolant (W_{cl}), C_{p} is the specific heat of water and the temperature difference between the stack inlet temperature (T_{in}) and the stack temperature (T_{st}).

$$\dot{\mathrm{Q}}_{\mathrm{cl}} = \mathrm{W}_{\mathrm{cl}} \mathrm{C}_{\mathrm{p}} (\mathrm{T}_{\mathrm{st}} - \mathrm{T}_{\mathrm{in}}) \quad (10)$$

where W_{cl} is coolant flow rate and C_{p} is specific heat of the coolant.

Here, circulating coolant serves as the primary cooling medium for the entire stack, with approximately 90 percent of the heat being extracted by it.

The stray heat loss of stack by its surface is proportional to stack temperature (T_{st}) and ambient temperature ($\mathrm{T}_{\mathrm{amb}}$).

$$\dot{\mathrm{Q}}_{\mathrm{loss}} = \frac{\mathrm{T}_{\mathrm{st}} - \mathrm{T}_{\mathrm{amb}}}{R_{\mathrm{int}}} \quad (11)$$

where R_{int} is thermal resistance.

III. DESIGN OF BF-STSMC FOR TEMPERTURE CONTROL OF A PEMFC

SMC [18] has emerged as a robust and effective technique for temperature control in PEMFC. SMC is also applied to other filed for the control like in [20-22]. But it has limitations when it comes to the system having unknown disturbances as the switching function gain is constant. The proposed strategy of BF-STSMC consists by increasing the gain until the moment when the sliding mode (SM) is reached, and then to fix the SM gain at this value, ensuring an ideal SM for some interval of time. When the disturbance grows, the SM can be lost, so the gain increases to reach it again. By harnessing the principles of sliding mode control integrated with super twisting algorithms, BF-STSMC offers a robust solution to address the nonlinear dynamics, uncertainties, and disturbances inherent in PEMFC systems. This advanced control strategy enables precise regulation of temperature within PEMFCs, ensuring optimal operating conditions for enhanced efficiency and durability. By swiftly driving the system states towards a designated sliding surface, BF-STSMC effectively suppresses temperature variations, mitigating the risk of thermal degradation and improving overall system performance. Through theoretical analysis and simulation studies, the efficacy of BF-STSMC in temperature control of PEMFCs has been demonstrated, showcasing its potential to advance the capabilities of PEMFC technology and facilitate its integration into various renewable energy applications.

Temperature tracking error (e) is defined as

$$e = T_{ref} - \mathrm{T}_{\mathrm{st}} \quad (12)$$

where T_{ref} is the constant reference temperature.

Sliding surface (S) is selected as:

$$S = e + K \int e \quad (13)$$

Equivalent control law can be achieved by differentiating eq (13) w.r.t time equating it to zero

$$\dot{S} = \dot{e} + ke = \dot{T}_{ref} - \dot{T}_{st} + k\left(T_{ref} - \mathrm{T}_{\mathrm{st}}\right) = 0$$

$$\dot{S} = \dot{T}_{ref} - \frac{\dot{\mathrm{Q}}_{\mathrm{tot}} - \mathrm{P}_{\mathrm{st}} - \mathrm{W}_{\mathrm{cl}} \mathrm{C}_{\mathrm{p}} (\mathrm{T}_{\mathrm{st}} - \mathrm{T}_{\mathrm{in}}) - \dot{\mathrm{Q}}_{\mathrm{loss}}}{m_{\mathrm{st}} C_{\mathrm{st}}} + k\left(T_{ref} - \mathrm{T}_{\mathrm{st}}\right) = 0 \quad (14)$$

Control law (u(t)):

Coolant flow rate (W_{cl}) serves as a regulatory mechanism in control strategies:

$$u(t) = u_{eq} + u_{sw} \quad (15)$$

where $\begin{cases} u_{eq} = \frac{-P_{st}-\dot{Q}_{loss}+\dot{Q}_{tot}-K*(Tref-T_{st})*m_{st}C_{st}}{C_p*(T_{st}-T_{in})} \\ u_{sw} = k|s|^{0.5}\,\mathrm{sgn}(s) + k\int sign(S) \end{cases}$

Barrier function forces the sliding variable to remain within the interior of the feasible region ($|S| < \varepsilon$) [18]. Considering system, for any $\varepsilon > 0$ and for $t \geq 0$, the inequality $|S| < \varepsilon$ holds via adaptive control gain.

Barrier function:

$$k = \begin{cases} \frac{|S|}{\varepsilon - |S|} & if\ k > \mu \\ \mu & if\ k \leq \mu \end{cases} \quad (16)$$

The benefit in using this adaptation which is ensure that the auxiliary variable belong to $|s(t)| < \varepsilon$. where μ & ε is a small positive constant which ensures the small value of $|s(t)|$ during stable operations with the smallest amplitude of the adaptive gain of positive semidefinite barrier function. Barrier function forces the solution to remain within the interior of the feasible region.

For a system to guarantee its stability, the condition of reaching must be verified. To analyse the stability of the controller we construct the Lyapunov function (V) :

$$V(S) = \frac{1}{2}S^2 \quad (17)$$

V is a positive definite function and taking derivative of this scalar function:

$$\dot{V}(S) = S\dot{S} = S\left(\dot{T}_{ref} - \frac{\dot{Q}_{tot}-P_{st}-(u_{eq}+u_{sw})C_p(T_{st}-T_{in})-\dot{Q}_{loss}}{m_{st}C_{st}} + k(T_{ref} - T_{st})\right) \quad (18)$$

For controller meets the stability requirement, $\dot{V}(S)$ must be negative definite which guarantees the asymptotic stability. This is shown using the Barbalat's lemma. Here our intention is to prove that the sliding surface $S \to 0$ as $t \to \infty$. This can be satisfied by meeting the three conditions of Barbalat's lemma.

(i) boundedness of S: we know that the sliding surface (S) is related to the error and its integral. Since the control law $u(t)$ includes both equivalent and switching terms, and the switching term is designed to ensure that $S(t)$ is driven toward zero, we expect that $S(t)$ will not grow unbounded. Moreover, by selecting the gains k and the control structure appropriately, the control input is designed to regulate the system within reasonable bounds, ensuring that both error and its derivative remain bounded, and thus, S remains bounded.

(ii) Uniform continuity of S: the time derivative of the sliding surface is bounded and smooth i.e. uniformly continuous if the disturbances ($d(t)$) and the system parameters remain within their physical limit.

(iii) The derivative of sliding surface $\dot{S}$ will converge to zero as time $t \to \infty$. The switching control term u_{sw}works to drive the sliding surface S to zero, ensuring that $\dot{S}$ decreases over time. As the sliding mode control ensures that trajectories are driven to the sliding surface $S = 0$, this implies that $S \to 0$ as $t \to \infty$. In sliding mode, once the system reaches the surface, the dynamics remain on it, further enforcing that $\dot{S} \to 0$.

IV. RESULTS AND SIMULATIONS

This section presents the outcomes of simulations conducted to evaluate the efficacy of two distinct control strategies—namely, PI and BF-STSMC in regulating the temperature of a PEMFC system. Table 2 shows the parameters considered for modeling PEMFC fuel cell.

Table 2. PEM Fuel cell model parameters.

Parameter	Symbol	Values
Rated power	P_{rated}	5 W
Number of cells	N	35
Thermal capacitance	$m_{st}C_{st}$	17.9 K J^0C^{-1}
Thermal Resistance	R_t	0.115^0CW^{-1}
Enthalpy of combustion for hydrogen	ΔH	285.5 $K\,J\,mol^{-1}$
Ambient temperature	T_{amb}	25^0C
Constants	K, μ, ε	1, 0.1, 0.03 (respectively)
Cell membrane area	A	232 cm^2

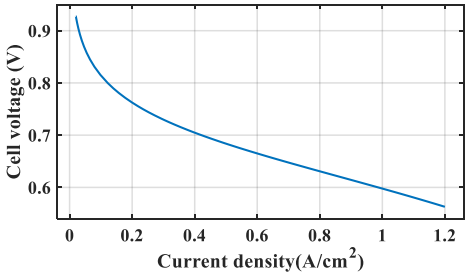


Figure 4: PEMFC output characteristic curve.

Fig. 4 shows the single PEMFC fuel cell output voltage and heat generations at operating temperatures 353 K. The PEMFC employs the Nafion-212 membranes. As shown in Fig. 2, when the fuel cell at operating temperatures, the polarization curves are similar [19] . When the current density increases to 1.2 A/cm2, the single fuel cell voltage drops from about 0.95 V to 0.55 V.

The primary objective was to maintain the system temperature at a predetermined setpoint of 75 degrees Celsius by modulating the flow rate of coolant, specifically water, in response to fluctuations in the current passing through the stack. Initial temperature of stack is 60 degree Celsius.

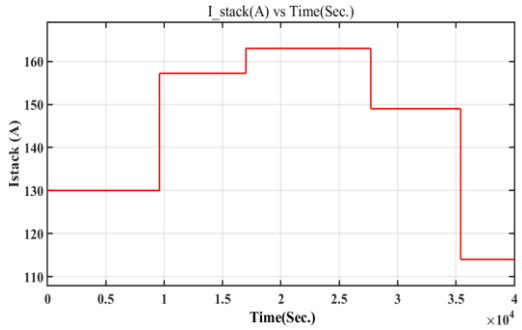


Figure 5: Stack current (I_{st}).

Figure 5 illustrates the current waveform through the stack. This waveform serves as the principal input to the control algorithms, directly influencing the thermal dynamics of the a PEMFC system.

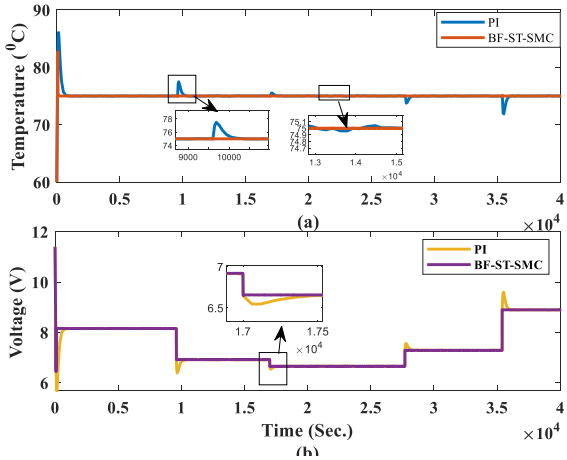


Figure 6: (a) Stack temperature (T_{st}) and Stack Voltage (V_{st}).

Figure 6(a) and Figure 6(b) provides a comparative analysis of the temperature regulation achieved and the voltage variations by the two distinct control methodologies. Notably, noticeable differences emerge in terms of settling time and oscillatory behavior in temperature. The PI controller, owing to its proportional and integral components, exhibits a relatively prolonged settling time compared to its counterparts. Conversely, the BF-STSMC approach demonstrates superior performance, achieving expedited settling times while maintaining stable temperature regulation.

V. CONCLUSIONS

This research paper has investigated some distinct control strategies, namely PI and BF-STSMC for regulating the temperature of a PEMFC system. The study focused on maintaining the temperature at a constant value of 75 degrees Celsius by adjusting the flow rate of coolant, which is water, in response to changes in current through the stack. Through simulation results, it was observed that each control strategy exhibited unique characteristics and performance outcomes. The PI controller demonstrated a longer settling time to reach the desired temperature due to its inherent integral action. In contrast, the BF-STSMC method demonstrated a quicker response with a reduced settling time while also avoiding chattering.

The findings suggest that the BF-STSMC strategy offers a favorable balance between rapid temperature regulation and stability compared to the PI. By leveraging its advanced sliding mode control mechanism, the BF-STSMC technique showcases promising potential for efficient temperature management in PEMFC systems, particularly in dynamic operating conditions where quick response.

REFERENCES

[1] M. Tawalbeh, S. Alarab, A. Al-Othman, and R. M. N. Javed, "The Operating Parameters, Structural Composition, and Fuel Sustainability Aspects of PEM Fuel Cells: A Mini Review," Fuels, vol. 3, no. 3, pp. 449–474, Aug. 2022.

[2] R. G. Bodkhe, R. L. Shrivastava, V. K. Soni, and R. B. Chadge, "A review of renewable hydrogen generation and proton exchange membrane fuel cell technology for sustainable energy development," Int J Electrochem Sci, vol. 18, no. 5, 2023, doi: 10.1016/j.ijoes.2023.100108.

[3] H. K. Esfeh and M. K. A. Hamid, "Temperature effect on proton exchange membrane fuel cell performance Part II: Parametric study," in Energy Procedia, Elsevier Ltd, 2014, pp. 2617–2620. doi: 10.1016/j.egypro.2014.12.261.

[4] M. A. Salam et al., "Effect of Temperature on the Performance Factors and Durability of Proton Exchange Membrane of Hydrogen Fuel Cell: A Narrative Review," Material Science Research India, vol. 17, no. 2, pp. 179–191, Sep. 2020, doi: 10.13005/msri/170210.

[5] H. K. Esfeh and M. K. A. Hamid, "Temperature effect on proton exchange membrane fuel cell performance Part II: Parametric study," in Energy Procedia, Elsevier Ltd, 2014, pp. 2617–2620. doi: 10.1016/j.egypro.2014.12.261.

[6] W.-J. Zou, and Y.-B. Kim. "Temperature control for a 5 kW water-cooled PEM fuel cell system for a household application." IEEE Access 7, 2019, pp. 144826-144835.

[7] M. Y. Silaa, M. Derbeli, O. Barambones, and A. Cheknane, "Design and Implementation of High Order Sliding Mode Control for PEMFC Power System," Energies (Basel), vol. 13, no. 17, Sep. 2020, doi: 10.3390/en13174317.

[8] J. H. Xu et al., "Sparrow search algorithm applied to temperature control in PEM fuel cell systems," Int J Hydrogen Energy, vol. 47, no. 94, pp. 39973–39986, Dec. 2022, doi: 10.1016/j.ijhydene.2022.09.141.

[9] X. Chen et al., "Temperature and voltage dynamic control of PEMFC Stack using MPC method," Energy Reports, vol. 8, pp. 798–808, Nov. 2022, doi: 10.1016/j.egyr.2021.11.271.

[10] V. Liso, M. P. Nielsen, S. K. Kær, and H. H. Mortensen, "Thermal modeling and temperature control of a PEM fuel cell system for forklift applications," in International Journal of Hydrogen Energy, Elsevier Ltd, May 2014, pp. 8410–8420. doi: 10.1016/j.ijhydene.2014.03.175.

[11] X. Chen et al., "Temperature and humidity management of PEM fuel cell power system using multi-input and multi-output fuzzy method," Appl Therm Eng, vol. 203, Feb. 2022, doi: 10.1016/j.applthermaleng.2021.117865.

[12] G. Li et al., "Feed-forward offset-free model predictive temperature control for proton exchange membrane fuel cell: An experimental study," ISA Trans, vol. 128, pp. 159–170, Sep. 2022, doi: 10.1016/j.isatra.2021.11.005.

[13] G. Li and Y. Li, “Temperature Control of PEMFC Stack Based on BP Neural Network,” 2016 4th International Conference on Machinery, Materials and Computing Technology, 2016. doi: 10.2991/icmmct-16.2016.270.
[14] Y. Li, H. Wang, and Z. Dai, “Using Artificial Neural Network to Control the Temperature of Fuel Cell,” in 2006 International Conference on Communications, Circuits and Systems, IEEE, Jun. 2006, pp. 2159–2162. doi: 10.1109/ICCCAS.2006.284926.
[15] J. Li, Y. Li, and T. Yu, “Distributed deep reinforcement learning-based multi-objective integrated heat management method for water-cooling proton exchange membrane fuel cell,” Case Studies in Thermal Engineering, vol. 27, p. 101284, Oct. 2021, doi: 10.1016/j.csite.2021.101284.
[16] L. Sun, G. Li, Q. S. Hua, and Y. Jin, “A hybrid paradigm combining model-based and data-driven methods for fuel cell stack cooling control,” Renew Energy, vol. 147, pp. 1642–1652, Mar. 2020, doi: 10.1016/j.renene.2019.09.048.
[17] M. J. Khan and M. T. Iqbal, “Modelling and analysis of electrochemical, thermal, and recetant flow dynamics for a PEM fuel cell system,” Fuel Cells, vol. 5, no. 4, pp. 463–475, Dec. 2005, doi: 10.1002/fuce.200400072.
[18] H. Obeid et al., “Barrier Function-Based Adaptive Integral Sliding Mode Control,” 2018 IEEE Conference on Decision and Control (CDC) : 17-19 Dec. 2018.
[19] L. Xing et al., “Thermal analysis and management of proton exchange membrane fuel cell stacks for automotive vehicle,” Int J Hydrogen Energy, vol. 46, no. 64, pp. 32665–32675, Sep. 2021, doi: 10.1016/j.ijhydene.2021.07.143.
[20] J. P. Singh and B. K. Roy, “Second order adaptive time varying sliding mode control for synchronization of hidden chaotic orbits in a new uncertain 4-D conservative chaotic system,” Trans. Inst. Meas. Control, pp. 1–14, 2017.
[21] J. P. Singh and B. K. Roy, “A new four-dimensional chaotic system with first Lyapunov exponent ≈ 22, hyperbolic curve and circular paraboloid types of equilibria and its switching synchronization by an adaptive global integral sliding mode control,” Chinese Phys. B, vol. 27, no. 4, pp. 040503–040517, 2018.
[22] A. Patel and J. P. Singh, “A Modified Sliding Mode Control for a Three-Parameter Fourth-Order Chaotic Model of a Power System,” 2022 IEEE 2nd Int. Conf. Sustain. Energy Futur. Electr. Transp. SeFeT 2022, no. August, pp. 1–5, 2022.